UDC 612.743

Y. RONG[1], D. HAO[1], X. HAN[2], Y. ZHANG[1], J. ZHANG[1], and Y. ZENG[1]

CLASSIFICATION OF SURFACE EMG USING WAVELET PACKET ENERGY ANALYSIS AND A GENETIC ALGORITHM-BASED SUPPORT VECTOR MACHINE

Received September 5, 2012.

The aim of our study was to recognize results of surface electromyography (sEMG) recorded under conditions of a maximum voluntary contraction (MVC) and fatigue states using wavelet packet transform and energy analysis. The sEMG signals were recorded in 10 young men from the right upper limb with a handgrip. sEMG signals were decomposed by wavelet packet transform, and the corresponding energies of certain frequencies were normalized as feature vectors. A back-propagation neural network, a support vector machine (SVM), and a genetic algorithm-based SVM (GA-SVM) worked as classifiers to distinguish muscle states. The results showed that muscle fatigue and MVC could be identified by level-4 wavelet packet transform and GA-SVM more accurately than when using other approaches. The classification correct rate reached 97.3% with sevenfold cross-validation. The proposed method can be used to adequately reflect the muscle activity.

Keywords: surface electromyography, wavelet packet transform, back-propagation neural network, support vector machine, genetic algorithm.

INTRODUCTION

Surface electromyography (sEMG) signals are the one-dimensional time-series signals obtained by bioelectrical changes on the skin surface induced by activity of the neuromuscular system. Surface EMG has significant advantages, such as non-invasive, real-time, and multitarget measurements. The sEMG signal can provide information about various aspects of muscle activity, including the number and firing rates of recruited motor units during voluntary isometric contraction. It reflects the functional status of the nerves and muscles and has been widely used in clinical medicine, sports medicine, and other fields [1]. Clinicians have used sEMG as a tool to diagnose certain motor disorders and to evaluate rehabilitation programs for patients. A vast literature regards the use of EMG to assess movement capabilities among patients suffered from stroke [2, 3]. Surface EMG from the patient's forearm was recorded in parallel with the local field potentials to accurately determine occurrences of Parkinson's disease-related tremor [4]. This approach was also applied to human-machine interfaces (HMIs) [5] and prosthetic control [6].

Force production involves the coordination of multiple muscles; the produced force levels can be attributed to electrical activities of the related muscles. Surface EMG displays distinct features with different exerted forces and fatigue states. Muscle fatigue is a reduction of the ability of the muscles to contract and develop force. Generally, localized muscle fatigue occurs after a prolonged and/or relatively strong muscle activity, when a muscle or a group of muscles are fatigued. The degree of muscle fatigue can be measured by assuming a relative maximal voluntary force lost during sustained contraction tasks as the equivalent [7, 8]. Some literature pointed out that muscle fatigue leads to recognizable degradation of the sEMG pattern. Many researchers emphasized that muscle fatigue is one of the risk factors for the musculoskeletal problem. Therefore, it is conceivable that through specific feature extraction and pattern recognition schemes, different types of muscle activity may be discernible via the sEMG signals.

Accurate and computationally efficient means of classifying sEMG signal patterns have been pursued in recent years. The time-domain algorithms for extracting features were not suitable because the

[1] College of Life Science and Bioengineering, Beijing, China.
[2] College of Applied Science, Beijing University of Technology, Beijing, China.
Correspondence should be addressed to D. Hao (e-mail: haodongmei@bjut.edu.cn) or Y. Zeng (e-mail: yjzeng@bjut.edu.cn).

absence of frequency resolution obscured the subtle presentation of complicated EMG signals. At the same time, the frequency-domain algorithms could not accurately represent the intrinsic property of biological signals due to the lack of time resolution [9]. Within recent years, a lot of studies utilized time-frequency methods to extract features, such as short-time Fourier transform (STFT), wavelet transform (WT), and wavelet packet transform (WPT) [6, 10, 11]. Short-time Fourier transform has the disadvantage of single resolution. Although WT can provide processing signals with multi-resolution, its frequency resolution decreases with wavelet scales increased; thus, this approach cannot provide enough information for pattern recognition. WPT can make up for the disadvantage of orthogonal wavelet transform. It not only improves the time resolution but also refines the gradually widened spectrum and demonstrated a favorable local quality [12].

Artificial neural networks (ANNs) and a support vector machines (SVMs) are feasible to classify sEMGs. ANN is formed of cells simulating the low-level functions of biological neurons [13]. It includes numerous neurons with nonlinear mapping ability. Neurons are linked to each other through the weight coefficient to form the adaptive nonlinear dynamic systems. In the Subasi's study, feedforward error back-propagation neural networks (BPNN)-based and wavelet neural networks (WNN)-based classifiers were developed and compared in relation to their accuracy in classification of EMG signals [13]. In a human–robot interface, EMG signals were also classified by a neural network to predict motion [14]. In addition, SVMs have gained wide acceptance due to their high generalization ability for a wide range of applications and better performance than other traditional learning machines [15]. Jianguo proposed a new recognition method of sEMG classification based on WT and SVM to classify the movement patterns, and the average recognition accuracy reached 98.75% [16]. Chattopadhyay presented a framework to measure the level of fatigue based on SVM in the wearable sensor technology [17].

In our investigation, we intended to distinguish sEMGs in maximum voluntary contraction (MVC) and the fatigue state with our self-developed system, which was available to study the cortico-muscular coherence. Such interaction was thought to mainly reflect the descending control from the primary motor cortex (M1) to the spinal motoneuronal pools [18]. EMG signals from three muscles of the forearm were collected while performing sustained MVCs until being fatigued. The features of sEMG signal were extracted by level-3 or level-4 wavelet packet transform, and sEMG energy in certain frequency band was calculated as well. After removing the abnormal data, BPNN and SVM classifiers were designed to discriminate sEMGs in MVC and the fatigue state. In addition, genetic algorithm (GA) was utilized to optimize parameters in the SVM.

METHODS

sEMG and a Force-Measure System. The self-developed measure system included three-channel sEMG and one-channel handgrip force detection circuits, as shown in Fig. 1. Ag-AgCl electrodes were used for sEMG recording to minimize the polarized voltage between the detection surface of the electrode and the skin. The preamplifier was composed of a differential amplification circuit and an instrument amplifier

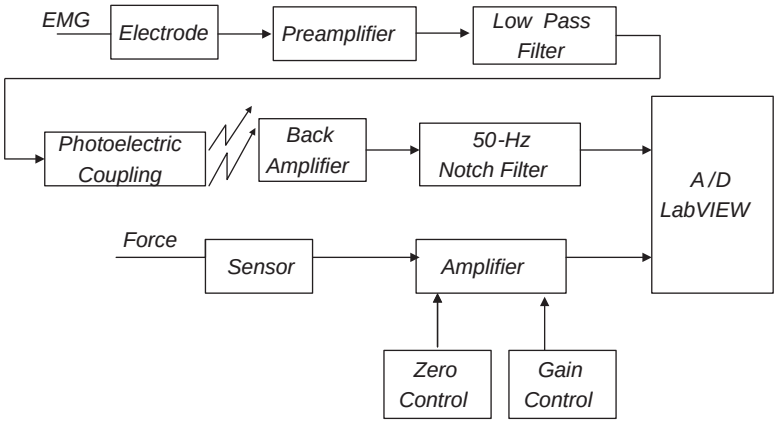

F i g. 1. EMG recording and handgrip force-measure system.

Р и с. 1. Система реєстрації ЕМГ та вимірювання сили стискання рукою.

AD620. The gain of the preamplifier was designed to 1000~1500, and its CMRR was 93 dB. A low-pass filter with the upper bandwidth cut-off frequency of 500 Hz could reduce the high-frequency disturbances. A photoelectric coupling circuit with TLP521 was designed to isolate the preceding and the following circuits from each other, so as to protect users. A reversed operation amplifier worked as the back-amplification unit with the gain 2 and the cut-off frequency 10 Hz. The ambient noise signal arising from the 50 Hz power sources may have amplitude that is one to three orders of magnitude greater than the sEMG signal; therefore, a dual-T network 50-Hz notch filter was used to remove the unwanted power line frequency. A force transducer (YJ-01, Anhui Zhongke Intelligent high-tech Co., Chinese Academy of Sciences) was used to detect the handgrip force with an error ≤1% of the full scale and a measurement range 0-500 N (≈0 to 50 kg force). Then, sEMG and force signals were sampled at 10^{-3} sec^{-1} with 12-bit of a PCI-6221 A/D acquisition card afforded by National Instruments (USA).

Examined Group and Mode of Recording. Ten healthy men aged from 20 to 24 years were recruited to participate in this experiment after giving their informed consents. The maximum voluntary contraction force of every subject was measured at the beginning of the experiment. The exerted force was displayed on a computer screen. Participants maintained MVC in a sitting position with the elbow joint at 100° until they felt exhausted and were no longer able to continue the contraction. The sustained contraction was terminated if the exerted force dropped by 10% or more for more than 3 sec. The maximal and sustained contraction forces were measured by a force transducer. sEMG signals were recorded from *mm. extensor digitorum* (*ED*), *extensor carpi ulnaris* (*ECU*), and *extensor carpi radialis brevis* (*ECRB*) with Ag-AgCl electrodes. A reference electrode was placed on the skin overlying the wrist joint to eliminate the common-mode interference on the body. Each subject was required to repeat the test three times. Fifty-six data sets having a stable force output lasting for more than 1 sec were selected for the subsequent analysis.

Feature Selection. Through analyzing the experimental data, it was noticed that the sEMG energy in fatigue increased in a low-frequency range and decreased in a high-frequency one compared with the non-fatigue state. Consequently, we created sEMG feature vectors with the energy of every frequency band of each muscle.

Wavelet packet transform. As an extension of the standard wavelet, WPT represents a generalization of multiresolution analysis and utilizes the entire family of sub-band decomposition to generate an overcomplete representation of the signals [6]. It uses a narrow window in the high-frequency domain and a wide window in the low-frequency domain. Therefore, it can provide good frequency resolution at all frequencies, and the noise components in a signal can be isolated, while important high-frequency transients can also be preserved [19]. WPT allows the original signal to be represented with various combinations of low- and high-frequency components [20], e.g.,

$$S = AAA3+DAA3+ADA3+DDA3+AAD3+ +DAD3+ADD3+DDD3. \quad (1)$$

It also could be defined as

$$S = AAA3+DAA3+ADA3+DDA3+D1, \quad (2)$$

where S is the original signal, and numbers 1 and 3 are the depth of a binary tree. A and D, respectively, stand for the low- and high-frequency components. S can also be expressed by a wavelet packet decomposition tree shown in Fig. 2.

Any node in the binary tree is labeled by its depth *j* and node number *p*. Each node (*j, p*) corresponds to a space W_j^p. The two wavelet packet orthogonal bases at the children nodes are defined by the recursive relations

$$W_j^{2p-1}(t) = \sum_{n=-\infty}^{\infty} h[n] W_{j-1}^p (n-2t) \quad (3)$$

and

$$W_j^{2p}(t) = \sum_{n=-\infty}^{\infty} g[n] W_{j-1}^p (n-2t), \quad (4)$$

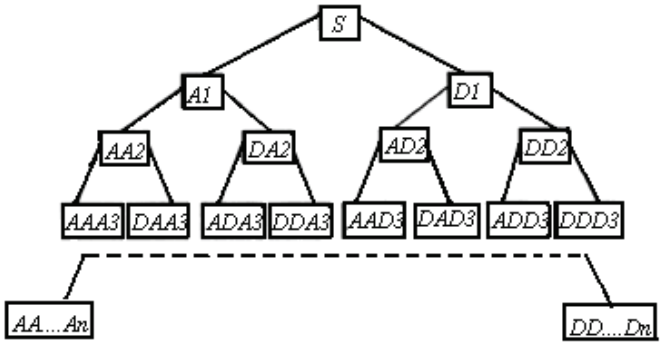

F i g. 2. Wavelet packet decomposition tree.

Р и с. 2. Дерево вейвлет-пакетної декомпозиції.

where $g(n) = (-1)^n h(1 - n)$, i.e., $g(n)$ is orthogonal with $h(n)$. This recursive splitting defines a binary tree of wavelet packet spaces where each parent node is divided into two orthogonal subspaces [6]. Hence, the wavelet packet transform of $x(t)$ can be calculated by the following recursive algorithm:

$$x_0^1(k) = x(t),\ x_j^{2p-1}(k) = Hx_{j-1}^p(k),$$
$$x_j^{2p}(k) = Gx_{j-1}^p(k),\quad x_{j-1}^p(k) = x_j^{2p-1}(k) + x_j^{2p}(k), \quad (5)$$

where j is the depth of the binary tree, and p is the number of the node.

Energy analysis. In our study, the energy of the pth frequency band in the jth layer E_j^p could be defined by the recursive relations:

$$E_j^p = \int \left| x_j^p(t) \right|^2 dt = \sum_{k=1}^{M} \left| d_{j,p}^k \right|^2, \quad (6)$$

where $d_{j,p}^k$ is the coefficient of the k-th discrete point of the decomposition signal $x_j^p(t)$, and M is the number of $x_j^p(t)$. The energy of the p band in the jth layer was normalized to obtain the relative value e_j^p according to formula

$$e_j^p = \frac{E_j^p}{\sum_{p=1}^{2^j} E_j^p}. \quad (7)$$

In order to further eliminate the individual discrepancy and reduce the number of feature vectors to optimize computation, the feature vector of one muscle S_j was constructed as formula

$$S_j = \left\{ \frac{e_j^p}{e_j^1}, p \in [2, 2^j] \right\}. \quad (8)$$

As is known, the activity of several muscles is coordinated to perform certain movements. The feature vector of each muscle can be combined together to characterize sEMG in a state.

Classification. Due to small sizes of the samples and the nonlinear feature vector, BPNN, SVM, and GA-SVM were designed in our study to compare the classification results.

Removal of the abnormal samples. Considering the existence of abnormal samples among the training data, e.g., noises with different variances, a method of detecting abnormal data based on support vector regression (SVR) was used [21]. SVR does not intend to eliminate an individual major error, while it considers the smooth of the regression curve entirety on the whole and distinguishes the abnormal data by comparing the regression value with the operational data [22]. All the samples could be distinguished into support vectors and non-support vectors, and the support vectors could be divided into boundary support vectors and non-boundary support vectors. Because the non-boundary support vectors or the abnormal samples were not from the same model with the boundary support vectors or the normal samples, therefore, they were located outside the normal scope.

In our study, the normal scope was set to [–0.82, 0.82]. Each component of the sample vectors was predicated with SVR, and a sample was regarded as abnormal when two components of the sample were outside the normal scope. The flowchart of abnormal data detection is shown in Fig. 3.

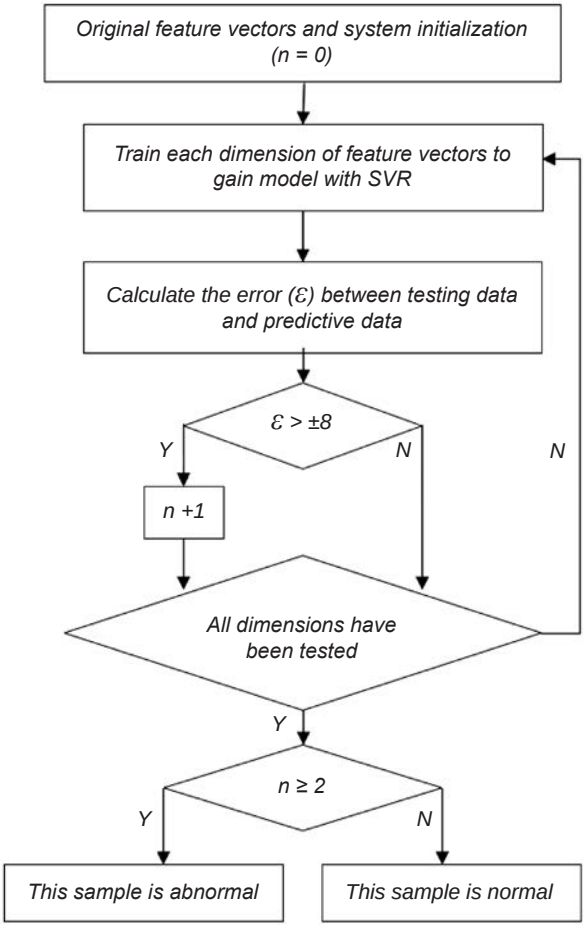

F i g. 3. Flowchart of abnormal data detection.

Р и с. 3. Схема виявлення аномальних даних.

Back-propagation neural network. Neural network can be applied in recognition and analysis of sEMG because of its parallel computing and adaptive learning abilities. Back-propagation neural network (BPNN) is a forward multilayer network, which uses the error back-propagation algorithm to train the network [23].

The BPNN structure was determined as *m*-*N*-1, in which there were *m* input nodes, and *m* was decided by the dimension of input vectors, one hidden layer with *N* nodes, and one output node. It was crucial to set the hidden-layer nodes because their number affects the neural network efficiency [20, 24]. *N* was usually decided by experience and trials in the study. If the input vectors were 3-dimensional, *N* could be 7 to 12; if the input vectors were 7-dimensional, *N* could be 6 to 20. The output was 1 for MVC and –1 for fatigue. The logsig and tansig sigmoid transfer functions were used in the hidden layer and the output layer, respectively, and the Levenberg–Marquardt (LM) learning algorithm was applied to training the network [25].

Support vector machine (SVM) and genetic algorithm (GA). SVM has been designed to minimize the structural risk; therefore, it has better performance than other techniques based on minimization of the empirical risk [9]. Applying the kernel function technology, a nonlinear problem in the input space is mapped to a high-dimensional space, and then a linear discriminant function is constructed in this high-dimensional space. The most commonly used kernel functions are linear, radial basis (rbf), polynomial (poly) and cubic spline (spline) data interpolation. Different forms of kernel functions can generate different SVMs. All the four kinds of kernel functions were tried in our SVM.

It is important to optimize the error penalty parameter (*C*) and kernel parameters (*g*) in the SVM. The genetic algorithm (GA) is a randomized search and optimization algorithm that it makes use of the population search method, fitting large-scale parallel process and possessing a global search function [26, 27]. The GA was utilized to search model parameters *C* and *g* in our study.

The flowchart of the recognition system showing feature selection, classification, and then conclusion is shown in Fig. 4.

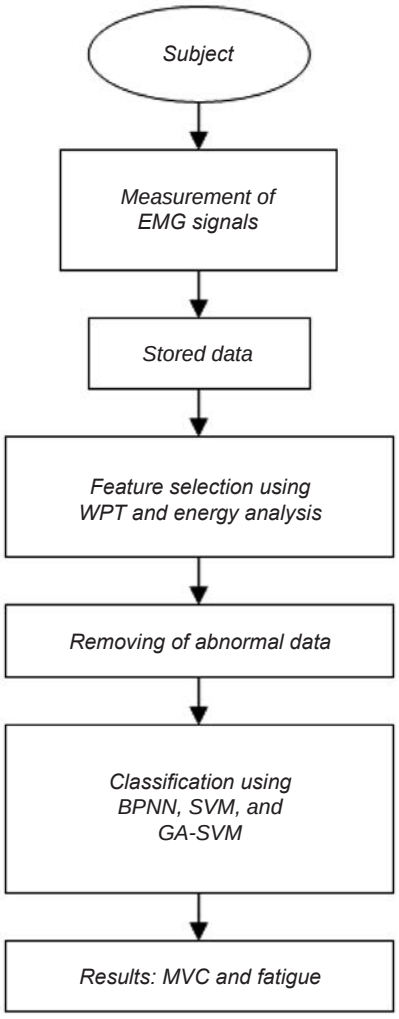

F i g. 4. Flowchart of the recognition system.

Р и с. 4. Схема системи розпізнавання.

RESULTS

Feature Selection. As was reported by Qi et al. [28], the muscle was supposed to be fatigued when the exerted force dropped by 10% or more for more than 3 sec during sustained contracting. Therefore, the grip force was taken into consideration to label the fatigue and MVC states. Figure 5 shows sEMGs and their power spectrum densities in MVC and fatigue; it can be seen that the sEMG energy was mainly distributed within the range of 5 to 150 Hz.

According to the frequency distribution, sEMG signals were decomposed with level-3 and level-4

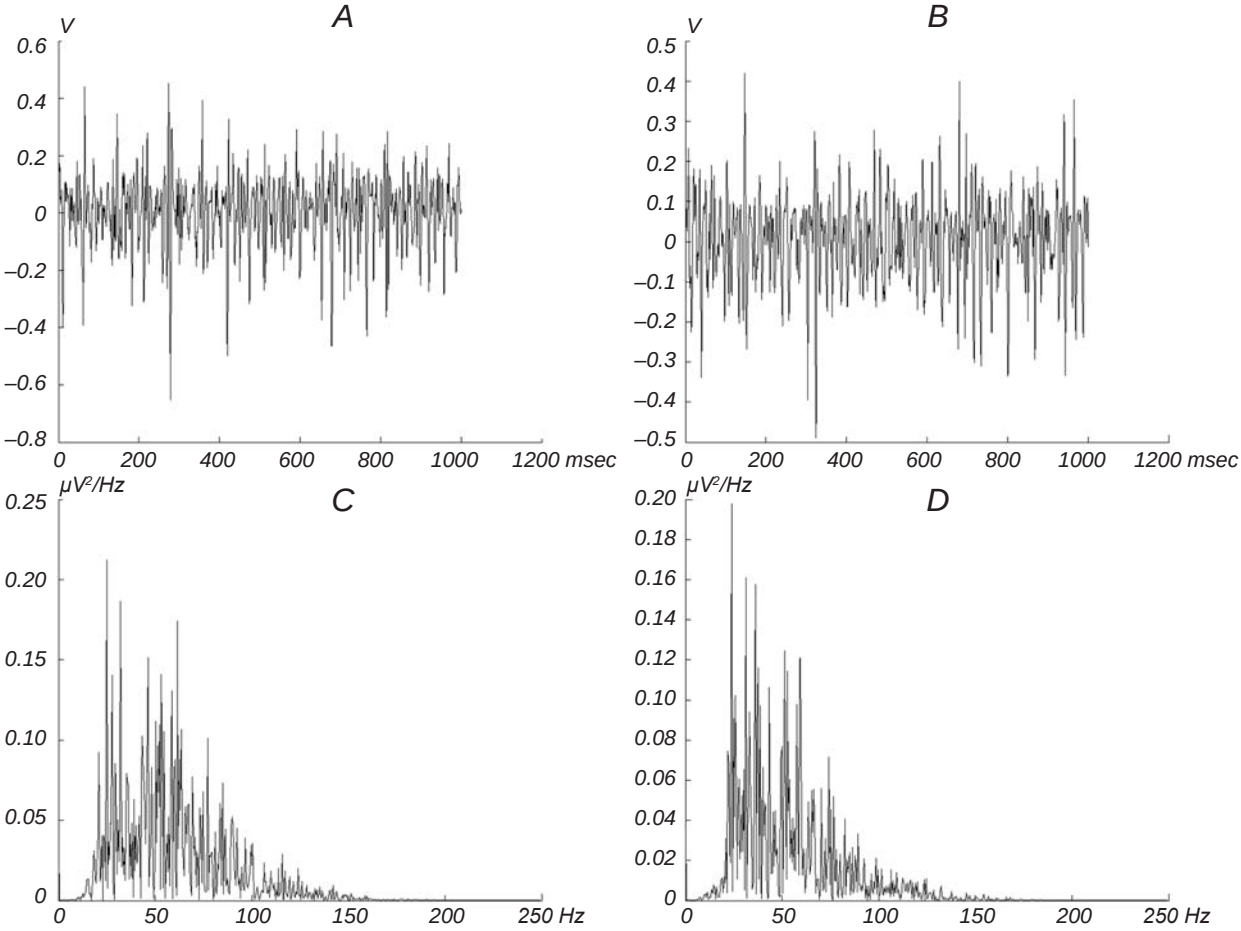

F i g. 5. Surface EMGs (sEMGs) and their power spectrum densities (PSDs) in different states. A and B) sEMGs in the state of maximum voluntary contraction (MVC) and fatigue, respectively. C and D) PSDs of sEMGs at MVC and in fatigue, respectively. In A and B: abscissa) time, msec; ordinate) sEMG amlitude, V. In C and D: abscissa) frequency, Hz; ordinate) PSD, mV^2/Hz.

Р и с. 5. "Поверхневі" електроміограми та їх спектральна щільність потужності в різних станах.

wavelet packet transforms, and the packets of {(3,1), (3,2), (3,3), (3,4)} and {(4,1), (4,2), (4,3), (4,4), (4,5), (4,6), (4,7), and (4,8)} were selected. The reconstructed signals of {(4,1), (4,2), (4,3), (4,4), (4,5), (4,6), (4,7), and (4,8)} are shown in Fig. 6. Two kinds of the feature vectors (3-dimension vector from level-3 WPT and 7-dimension vector from level-4 WPT) were composed of the normalized energies of the wavelet decomposition.

Removal of Abnormal Samples. As is shown in Fig. 7, each component of the sample vectors was used to construct a model with SVR. In the regression estimation, the residual of each component was obtained by calculating the difference between the model output and the sample. If the residuals of two components were out of the normal scope (tube), the sample was regarded as abnormal and eliminated. According to this model, 7 samples were removed and 21 samples were reserved from totally 42 samples for MVC and fatigue.

Classification. All samples were randomly partitioned into seven subsamples with k samples each (k = 8 or 6 before or after removal of the abnormal). Among the seven subsamples, one subsample was used as validation data for testing the model, and the other six subsamples were used as training data. The training data and testing data were then applied to the designed classifier. The cross-validation process was then repeated seven times, with each of the seven subsamples used only once as the validation data. The seven results from the folds then were averaged to produce a single estimate. The advantage of this

TABLE 1. Recognition Result of SVM with Two Kinds of Feature Vectors

SVM-результат розпізнавання з двома типами векторів особливостей

SVM classification accuracy	Kernel functions			
	linear	polynomial	radial basis	cubic spline
Before removal of the abnormal samples				
Level-3 WPT and SVM (%)	57.14	64.29	64.29	53.57
Level-4 WPT and SVM (%)	66.07	66.07	64.29	64.29
After removal of the abnormal samples				
Level-4 WPT and GA-SVM (%)	78.57	83.33	97.62	28.57

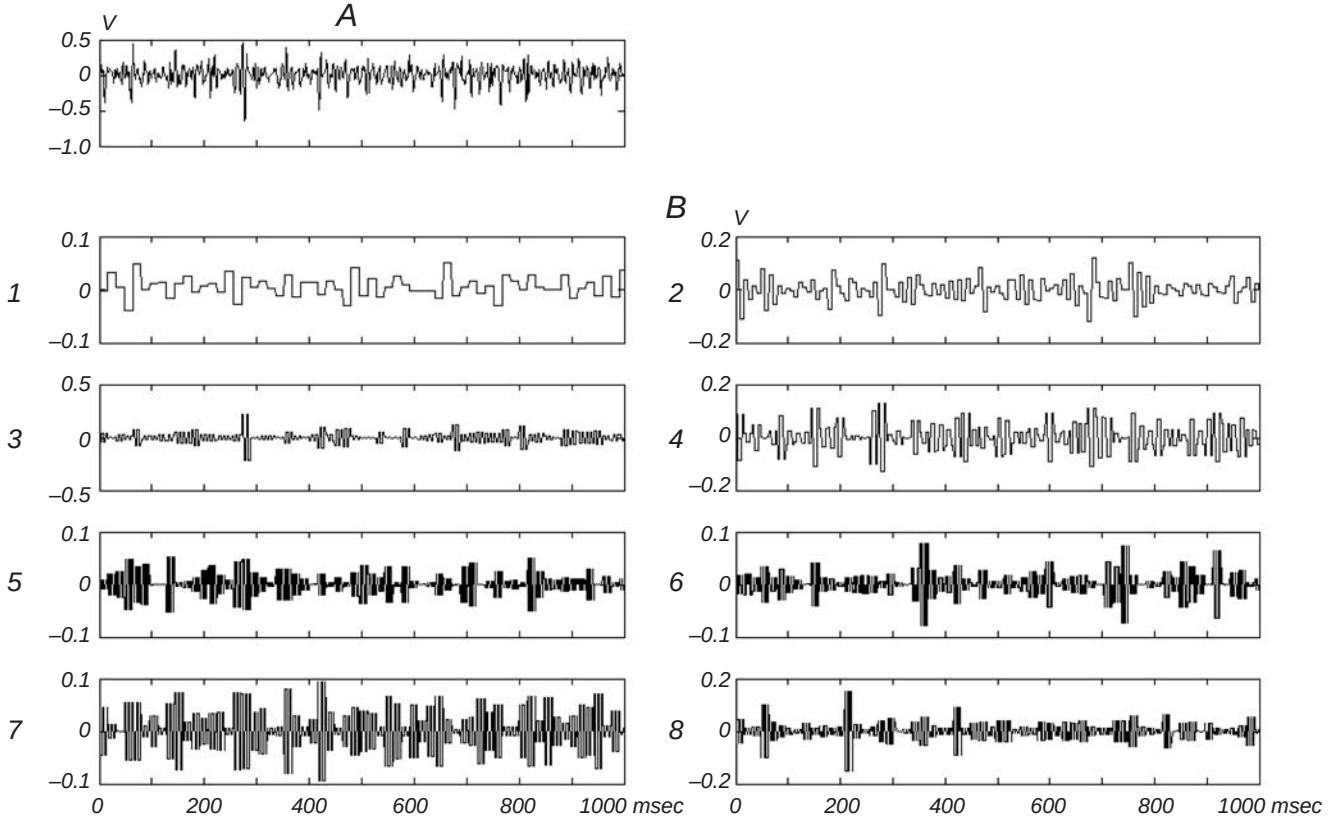

F i g. 6. Original sEMG (A) and eight low-frequency bands (B). In B, stands for sEMG of different frequency bands (Hz): 0-31.25 (1), 31.25-62.5 (2), 62.5-93.75 (3), 93.75-125 (4), 125-156.25 (5), 156.25-187.5 (6), 187.5-218.75 (7), and 218.75-250 (8). The bandwidth of each signal was 31.25 Hz. Abscissa) Time, msec; ordinate) amplitude of sEMG, V.

Р и с. 6. Оригінальна „поверхнева" електроміограма (*А*) та вісім низькочастотних смуг (*Б*).

method over repeated random subsampling is that all observations are used for both training and validation, and each observation is used for validation exactly once.

The BPNN recognition rate before and after removal of the abnormal samples is shown in Fig. 8, while the SVM classification accuracy before and after these procedure is shown in Table 1.

Figure 8A shows that BPNN could acquire a higher correct rate with the 7-dimensional vector (produced by level-4 WPT) than with the 3-dimensional vector (produced by level-3 WPT), and the best result was 87.5% with 15 hidden nodes. After removing of the abnormal samples, the accuracy was further improved with the 7-dimensional vector produced by level-4 WPT (compare Fig. 8A and B).

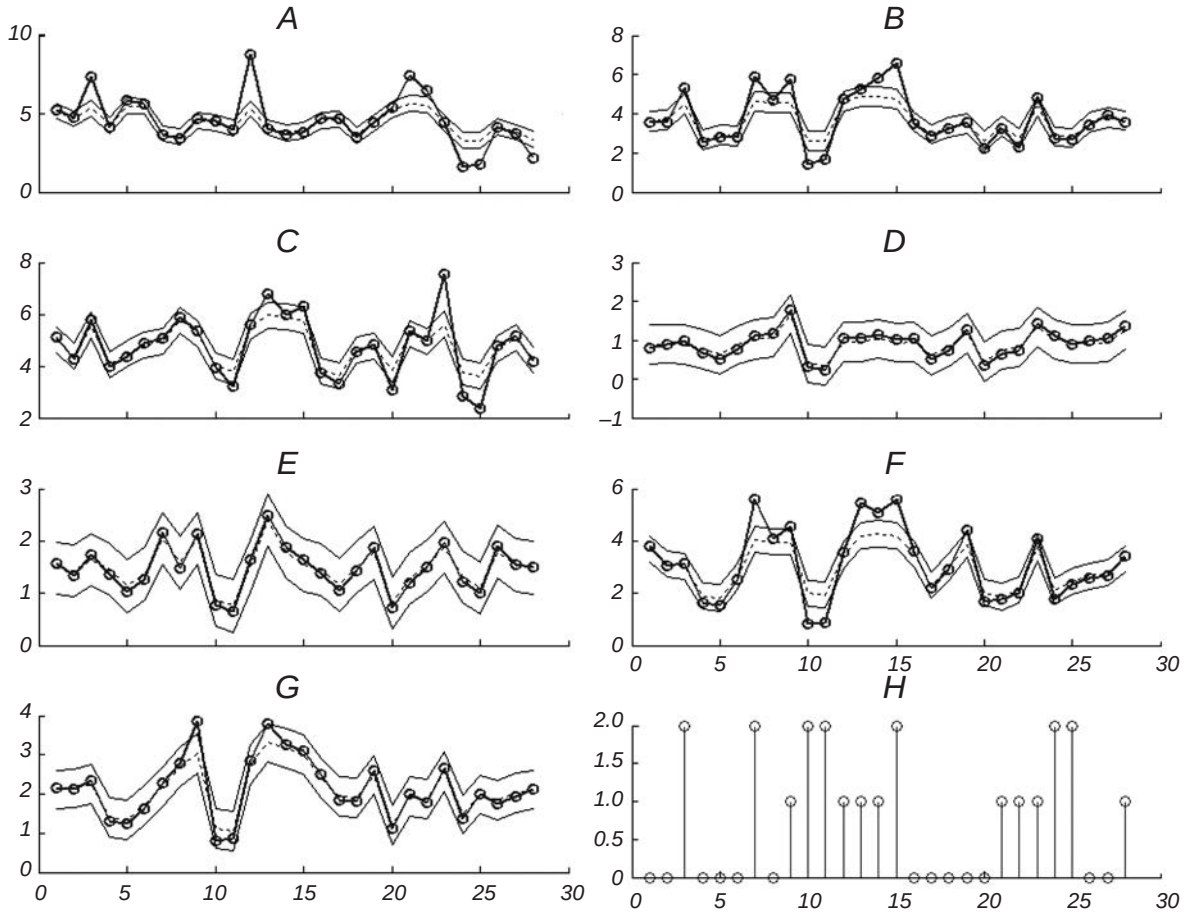

F i g. 7. Check feature vectors of samples in MVC. A–G) Regression comparisons of the first to the seventh dimension of the feature vectors. Dotted lines are regression results, solid lines are edges of the normal scope, and circles mean actual samples. Abscissa) Number of samples; ordinate) amplitude of the testing data and predictive data. H) Abnormal dimension number of the feature vectors. Abscissa) Number of the samples; ordinate) abnormal dimension number.

Р и с. 7. Вектори особливостей зразків у стані максимального довільного скорочення.

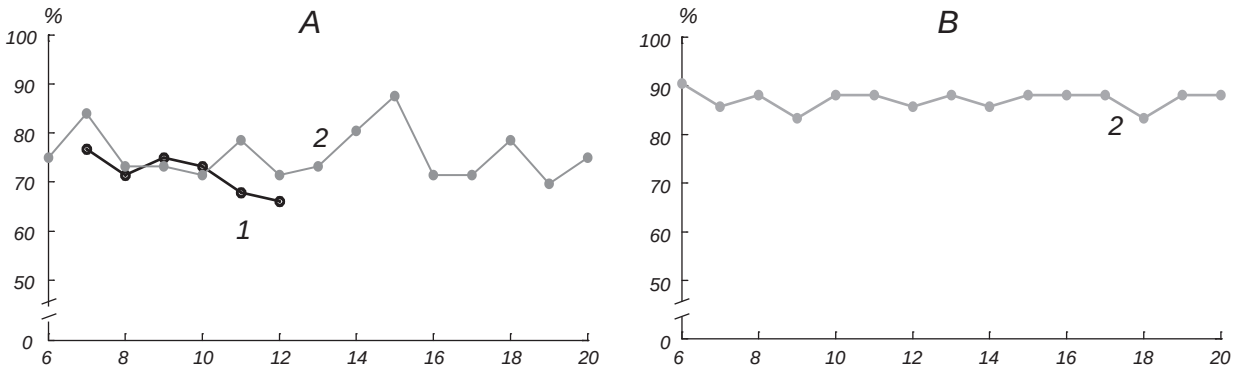

F i g. 8. Recognition result of BPNN with different hidden nodes. A) Before removal of the abnormal samples; B) after this procedure. Level-3 WPT produced 3-dimensional input vectors (1); hidden layer node was 7 to 12. Level-4 WPT produced 7-dimensional input vectors (2); hidden layer node was 6 to 20. Abscissa) Number of hidden layer nodes; ordinate) recognition rate, %.

Р и с. 8. BPNN-результат розпізнавання з різними прихованими вузлами.

Table 1 shows that, with SVM, the 7-dimensional vector produced by level-4 WPT also had better classification than the 3-dimensional vector produced by level-3 WPT. After removal of the abnormal samples, the accuracy was greatly improved, and the best result was 97.62% with GA-SVM using the rbf kernel function.

DISCUSSION

This study proposed the sEMG feature extraction method based on WPT and energy analysis according to the distinct frequency characteristics of sEMGs from the *ED*, *ECU*, and *ECRB* muscles in the MVC and fatigue states. Then, the classification accuracy of BPNN, SVM, and GA-SVM were compared; it has been demonstrated that GA-SVM had higher recognition ability than the other two methods in distinguishing the MVC and fatigue states of sEMG. GA-SVM is more intelligent and time-saving because GA has characteristics of self-organization, self-learning, and self-adaptation, and it can discover the environment feature to search those based on changes of the environment automatically. This algorithm might be used to solve complicated and unstructured problems [26].

Compared with our previous research, this paper introduced energy analysis in different frequencies based on WPT. As is shown in Fig. 5, it was found that the sEMG energy increased in the low-frequency and decreased in the high-frequency ranges when muscles were fatigued compared with MVC, which is consistent with the other study [29]. It occurs possibly because the firing rates of motor units decreased and caused the power spectrum of sEMG signal to compress toward a lower-frequency range during the fatigue state. Therefore, the energies within certain frequency ranges were selected and normalized to act as feature vectors. In this paper, 3-dimensional and 7-dimensional feature vectors of sEMG were acquired with level-3 WPT and level-4 WPT. According to the classification results, it suggested that the 7-dimensional feature vectors from level-4 WPT were more suitable for classification than the 3-dimensional ones. Although the feature vectors from higher-level WPT had more detailed information, they reduced the classification accuracy, possibly because a part of the information was useless for classification.

In this study, we found that the BPNN output was sensitive to initial weights and thresholds due to the small sample size. To some extent, increasing the sample size can improve the recognition rate. However, excessive samples might cause BPNN over-fitting. Consequently, BPNN was trained in our study more than 20 times by the same training set, and then the results were analyzed by statistics. The BPNN was determined by the output appearing to the greatest extent. For the node selection in the hidden layer, our experiments showed that the hidden-layer nodes had a significant impact on the performance of the neural network [23]. If too few nodes exist, each category could not be separated by the network, and if too many nodes exist, the operation was too big (there may be "over-learning"); therefore, the system performance and efficiency must be taken into full consideration to determine the hidden-layer nodes. The correct rate of BPNN was related to both the feature vectors and neurons in the hidden layer.

Removal of the abnormal samples is a key event to provide effective classification [21, 22, 30]. According to our results, the recognition rate of BPNN was greatly improved after removal of the anomalies, and the influence of the hidden-node number was reduced (Fig. 8B). The highest rate was 90.73%, and the lowest rate was 83.33% with BPNN. For SVM, the best result was 97.62% with GA-SVM (Table 1), which indicated that, after removing the abnormal parameters, optimization with GA greatly improved the SVM performance.

In summary, the feature vectors based on wavelet packet transform and energy analysis are able to reflect the major characteristics of sEMG and can be used to distinguish sEMG in MVC and fatigue states. The SVM was suitable for classification of small-sized and nonlinear samples. Furthermore, GA applied to SVM can optimize the parameters. Therefore, higher classification accuracy was achieved by combining the appropriate feature extraction and the classifier design. At present, however, the proposed methods were only used to classify two sEMG patterns. EMGs with 25, 50, and 75% MVC were collected in our experiments besides the MVC and fatigue states. Multi-pattern sEMGs will be recognized in the further study.

Acknowledgments. This work was supported by the National Natural Science Foundation of China, No. 81071231 and No. 30670543.

Я. Рон[1], Д. Хао[1], Кс. Хан[2], Я. Жан[1], Дж. Жан[1], Я. Зен[1]

КЛАСИФІКАЦІЯ РЕЗУЛЬТАТІВ „ПОВЕРХНЕВОЇ" ЕЛЕКТРОМІОГРАФІЇ З ВИКОРИСТАННЯМ ПАКЕТНОГО ВЕЙВЛЕТ-АНАЛІЗУ ЕНЕРГІЇ ТА МАШИНИ ОПОРНИХ ВЕКТОРІВ, БАЗОВАНОЇ НА ГЕНЕТИЧНОМУ АЛГОРИТМІ

[1] Коледж наук про життя та біоінженерії, Пекін (Китай).
[2] Коледж прикладних наук Пекінського Технологічного університету (Китай).

Р е з ю м е

Ціллю нашого дослідження була розробка прийомів розпізнавання результатів електроміографічних відведень за допомогою поверхневих електродів (пЕМГ) в умовах розвитку максимального довільного скорочення та станів втоми; використовували пакетне вейвлет-перетворення та аналіз енергії. Сигнали пЕМГ піддавалися декомпозиції із застосуванням пакетного вейвлет-перетворення, і відповідні оцінки енергії певних частот нормувались як вектор ознак. Нейронна мережа із зворотним проведенням, машина опорних векторів (SVM) та SVM, базована на генетичному алгоритмі (GA-SVM), працювали як класифікатори, що розпізнавали стани м'язів. Отримані результати показали, що стани м'язової втоми та максимального довільного скорочення можуть бути ідентифіковані за допомогою пакетного вейвлет-перетворення 4-го рівня точніше, ніж у разі застосування інших підходів. Рівень коректності класифікації при семиразовій кросвалідизації сягав 97.3 %. Запропонований метод може бути використаний для адекватного відображення м'язової активності.

REFERENCES

1. C. Frigo, M. Ferrarin, and W. Frasson, "EMG signals detection and processing for on-line control of functional electrical stimulation," *J. Electromyogr. Kinesiol.*, **10**, 351-360 (2005).
2. M. S. Fimland, P. M. Maen, T. Hill, et al., "Neuromuscular performance of paretic versus non-paretic plantar flexors after stroke," *Eur. J. Appl. Physiol.*, **111**, No. 12, 3041-3049 (2011).
3. T. H. Sande, S. Leistne, and F. Geisle, "Characterization of motor and somatosensory function for stroke patients," *Physiol. Meas.*, **32**, 1737-1746 (2011).
4. D. Wu, K. Warwick, and Z. Ma, "Prediction of Parkinson's disease tremor onset using a radial basis function neural network based on particle swarm optimization," *Int. J. Neural Syst.*, **20**, No. 2, 109-116 (2010).
5. M. R. Ahsan, M. I. Ibrahimy, and O. Khalifa, "Hand motion detection from EMG signals by using ANN based classifier for human computer interaction," in: *Proceedings of the 4th International Conference on Modeling, Simulation and Applied Optimization* (*ICMSAO*, 2011), pp. 1-6.
6. H. B. Xie, Y. P. Zheng, and J. Y. Guo, "Classification of the mechanomyogram signal using a wavelet packet transform and singular value decomposition for multifunction prosthesis control," *Physiol. Meas.*, **30**, 441-457 (2009).
7. Y. Soo, M. Sugi, M. Nishino, et al., "Quantitative estimation of muscle fatigue using surface electromyography during static muscle contraction," in: *Conf. Proc. IEEE Eng. Med. Biol. Sci.* (2009), pp. 2975-2978.
8. J. Z. Liu, B. Yao, and V. Siemionow, "Fatigue induces greater brain signal reduction during sustained than preparation phase of maximal voluntary contraction," *Behav. Brain Res.*, **1057**, 113-126 (2005).
9. Z. G. Yan, Z. Z. Wang, and X. M. Ren, "Joint application of feature extraction based on EMD-AR strategy and multi-class classifier based on LS-SVM in EMG motion classification," *J. Zhejiang Univ. Sci.*, **8**, No. 8, 1246-1255 (2007).
10. J. U. Chu, I. Moon, and Y. J. Lee, "A supervised feature-projection-based real-time EMG pattern recognition for multifunction myoelectric hand control," *IEEE Trans. Mechatronics*, **12**, 282-290 (2007).
11. R. Behroozmand and F. Almasganj, "Optimal selection of wavelet-packet-based features using genetic algorithm in pathological assessment of patients' speech signal with unilateral vocal fold paralysis," *Comput. Biol. Med.*, **37**, 474-485 (2007).
12. H. B. Xie, H. Huang, and Z. Z. Wang, "Wavelet packet transformation feature extraction and surface EMG signal classification," *Med. Equipment J.*, **24**, 7-10 (2003).
13. A. Subasi, M. Yilmaz, and H. R. Ozcalik, "Classification of EMG signals using wavelet neural network," *J. Neurosci. Methods*, **156**, 360-367 (2006).
14. N. Bu, M. Okamoto, and T. Tsuji, "A hybrid motion classification approach for EMG-based human-robot interfaces using bayesian and neural networks," *IEEE Trans. Robot*, **25**, 502-511 (2009).
15. S. Koçer, "Classifying myopathy and neuropathy neuromuscular diseases using artificial neural networks," *Int. J. Patt. Recogn. Artif. Intell.*, **24**, 791-807 (2010).
16. J. G. Cui, X. Wang, Z. H. Li, et al., "Application of support vector machine in pattern classification of surface EMG," *J. Northeastern Univ. Nat. Sci.* (China), **27**, 280-283 (2006).
17. R. Chattopadhyay, G. Pradhan, and S. Panchanathan, "Towards fatigue and intensity measurement framework during continuous repetitive activities," in: *Instrumentation and Measurement Technology Conference (I2MTC), 2010 IEEE* (2010), pp. 1341-1346.
18. F. Meng, K. Y. Tong, S. T. Chan, et al., "Study on connectivity between coherent central rhythm and electromyographic activities," *J. Neural Eng.*, **5**, 324-332 (2008).
19. M. S. Hussain, M. B. Reaz, F. Mohd-Yasin, et al., "Electromyography signal analysis using wavelet transform and higher order statistics to determine muscle contraction," *Expert Systems*, **26**, No. 1, 35-48 (2009).
20. B. Cheng and G. Y. Liu, "Emotion recognition from surface EMG signal using wavelet transform and neural network," *J. Comput. Applic.*, **28**, 333-337 (2008).
21. W. T. Mao, L. L. Dong, and G. Zhang, "Weighted solution path algorithm of support vector regression for abnormal data," in: *Proceedings of the 19th International Conference on Pattern Recognition*, *ICPR 2008*, (2008), pp. 2348-2351.
22. L. Wang, R. Q. Zang, W. Sheng, et al., "Regression forecast and abnormal data detection based on support vector regression," in: *Proceedings of the CSEE*, **29**, 92-96 (2009).
23. S. X. Yang and G. Y. Yang, "Emotion recognition of EMG based on improved L-M BP neural network and SVM," *J. Software*, **6**, 1529-1536 (2011).

24. R. Setiono, B. Baesens, and C. Mues, “Rule extraction from minimal neural networks for credit card screening,” *Int. J. Neural Syst*., **21**, 265-276 (2011).
25. J. P. Florido, H. Pomares, and I. Rojas, “Generating balanced learning and test sets for function approximation problems,” *Int. J. Neural Syst*., **21**, 247-263 (2011).
26. M. Y. Zhao, J. Ren, L. P. Ji, et al., “Parameter selection of support vector machines and genetic algorithm based on change area search,” *Neural Comput. Applic*., **21**, 1-8 (2012).
27. X. H. Lin, Q. C. Wang, P. Y. Yin, et al., “A method for handling metabonomics data from liquid chromatography/ mass spectrometry: combinational use of support vector machine recursive feature elimination, genetic algorithm and random forest for feature selection,” *Metabolomics*, **7**, No. 4, 549-558 (2011).
28. Q. Yang, Y. Fang, C. K. Sun, et al., “Weakening of functional corticomuscular coupling during muscle fatigue,” *Brain Res*., **1250**, 101-112 (2009).
29. G. Wang, X. M. Ren, L. Li, et al., “Multifractal analysis of surface EMG signals for assessing muscle fatigue during static contractions,” *J. Zhejiang Univ. Sci*., **8**, 910-915 (2007).
30. A. Kavitha, C. M. Sujatha, and S. Ramakrishnan, “Prediction of spirometric forced expiratory volume (FEV1) data using support vector regression,” *Measurement Sci. Rev*., **10**, No. 2, 63-67 (2010).